

EquiFlow: Equivariant Conditional Flow Matching with Optimal Transport for 3D Molecular Conformation Prediction

Qingwen Tian^{1,2*}, Yuxin Xu^{2*}, Yixuan Yang², Zhen Wang², Ziqi Liu^{2,3},
Pengju Yan^{2†}, Xiaolin Li^{2†}

¹Zhejiang University of Technology

²HIM, Chinese Academy of Sciences

³University of Chinese Academy of Sciences

tqw@zjut.edu.cn, xux@live.ca, yangyixuan@him.cas.cn, wangzhen@him.cas.cn, liuziqi22@mails.ucas.ac.cn,
yanpengju@gmail.com, xiaolinli@ieee.org

Abstract

Molecular 3D conformations play a key role in determining how molecules interact with other molecules or protein surfaces. Recent deep learning advancements have improved conformation prediction, but slow training speeds and difficulties in utilizing high-degree features limit performance. We propose EquiFlow, an equivariant conditional flow matching model with optimal transport. EquiFlow uniquely applies conditional flow matching in molecular 3D conformation prediction, leveraging simulation-free training to address slow training speeds. It uses a modified Equiformer model to encode Cartesian molecular conformations along with their atomic and bond properties into higher-degree embeddings. Additionally, EquiFlow employs an ODE solver, providing faster inference speeds compared to diffusion models with SDEs. Experiments on the QM9 dataset show that EquiFlow predicts small molecule conformations more accurately than current state-of-the-art models.

Introduction

3D molecular conformation prediction involves using computational methods and deep learning algorithms to determine the 3D spatial arrangement of molecules. In this context, atoms are represented by their Cartesian coordinates, and the 3D conformations of a molecule are critical for understanding its functionality, reactivity, and physical properties. The 3D conformations of a molecule dictate how it interacts with other molecules or protein surfaces, thereby influencing its chemical activity and function. This prediction has broad applications in computational drug and material design (Thomas et al. 2018; Gebauer et al. 2022; Jing et al. 2020; Batzner et al. 2022).

Traditional methods for predicting molecular conformations, such as those based on classical force fields (Wang et al. 2004) or quantum mechanical calculations, are accurate but computationally intensive and difficult to apply to large datasets. Additionally, methods like molecular dynamics or Markov Chain Monte Carlo are prohibitively expensive for large molecules, often requiring extensive runtime

to produce reliable results and may not resolve molecular symmetry issues.

Recently, deep learning has achieved significant advancements in fields such as image recognition and natural language processing. Consequently, more researchers are now exploring its application in molecular conformation prediction. The success of deep learning is largely attributed to its ability to employ structural symmetry. For instance, convolutional neural networks (CNNs) can process 2D images and recognize patterns efficiently irrespective of their positions, highlighting the importance of translational equivariance. Similarly, in processing 3D atomic graphs for molecules, the relevant inductive bias pertains to the 3D Euclidean group $E(3)$, which encompasses equivariance under operations involving translation, rotation, and reflection (Liao and Smidt 2023). As a result, certain properties of atomic systems should remain invariant under specific transformations. For example, when a system rotates, associated physical quantities like forces must rotate accordingly. To address this requirement, neural networks with invariance and equivariance properties have been developed. These networks have proven to be efficient tools for handling complex atomic graph data by effectively integrating these geometric principles.

In invariant neural networks, researchers aim to extract information such as distances and angles from 3D graph data that remain unchanged under rotations and translations, thereby enhancing the representation capability of the graphs (Simm and Hernandez-Lobato 2020; Xu et al. 2021; Shi et al. 2021; Ganea et al. 2021). These methods avoid directly modeling complex atomic coordinates by exploiting intermediate geometric variables that are invariant to rotations and translations. However, reliance on these intermediate variables may restrict the model’s flexibility and limit its applicability during both training and inference. Therefore, directly modeling atomic coordinates while maintaining translational and rotational invariance becomes an ideal solution (Xu et al. 2022), necessitating the use of equivariant neural networks. In the task of 3D molecular modeling, researchers have achieved significant results by constructing equivariant graph neural networks to predict or generate 3D molecular conformations. For instance, inspired by the dif-

*These authors contributed equally.

†Corresponding author.

fusion process in classical non-equilibrium thermodynamics, GeoDiff (Xu et al. 2022) models each atom as a particle and learns to simulate the diffusion process (from noise distribution to stable conformations) as a Markov chain to predict 3D molecular conformations. However, diffusion models (DMs) require substantial computational resources during both training and inference. Torsional Diffusion (Jing et al. 2022) addresses this issue by predicting the hypertorus on the torsion angles of each 3D molecular conformation instead of directly predicting their atomic coordinates. This method, however, relies on RDKit to generate rigid substructures for each molecule, hence it is not an end-to-end model. Inspired by recently proposed flow matching models (Lipman et al. 2023), EquiFM (Song et al. 2024) employs a novel flow matching training objective for geometric generation modeling in molecular generation. It utilizes Equivariant Graph Neural Networks (EGNN) (Satorras, Hoogeboom, and Welling 2021) to parameterize the vector field, trained via flow matching to satisfy translational and rotational equivariance constraints. However, these methods often rely on constructing equivariant graph neural networks based on low-degree features, limiting the benefit from information-rich high-degree features.

To avoid these limitations, we propose EquiFlow, an equivariant conditional flow matching (CFM) model with optimal transport (OT) for 3D molecular conformation prediction. EquiFlow is the first method to apply CFM to molecular conformation prediction, leveraging the efficient training and inference capabilities of CFM. It integrates a modified Equiformer model to encode Cartesian molecular conformations, fully adopting atomic type features and bond features, and facilitating effective interaction with higher-degree molecular features. Moreover, EquiFlow leverages an ODE solver, thereby facilitating more rapid inference speeds in comparison to DMs that utilize SDE. The main contributions of this work are as follows:

- Training the model with an OT flow objective that directly predicts the vector field around the atomic coordinates of molecules, resulting in stable and efficient training, high accuracy, and excellent diversity.
- Encoding Cartesian molecular conformations with modified Equiformer, leveraging atomic type and bond features, enabling effective interaction with higher-degree molecular features, and ensuring translational and rotational equivariance.
- Introducing the use of OT-CFM for the first time in the task of 3D molecular conformation prediction, providing a novel approach that combines optimal transport theory with flow matching to significantly improve the performance of conformation prediction models.

Related Works

Diffusion Model and Conditional Flow Matching

DMs (Sohl-Dickstein et al. 2015; Song and Ermon 2019; Ho, Jain, and Abbeel 2020) have recently achieved success in high-dimensional statistics (Rombach et al. 2022),

language modeling (Li et al. 2022), and equivariant representations (Hoogeboom et al. 2022). In the 3D molecular field, GeoDiff (Xu et al. 2022) and EDM (Hoogeboom et al. 2022) adopt DMs to learn score-based models for predicting molecular conformations. However, these approaches often face challenges such as unstable probability dynamics and inefficient sampling, which hinder their overall effectiveness. Torsional Diffusion (Jing et al. 2022) addresses these issues by decomposing molecules into rigid substructures, thereby reducing the computational burden to calculating only the torsion angles that connect these substructures. Despite its advantages, this method requires the pre-computation of rigid substructures, which can be a limitation for certain applications.

Normalizing flows (NFs) (Tabak and Vanden-Eijnden 2010; Tabak and Turner 2013; Rezende and Mohamed 2015; Papamakarios et al. 2021) are powerful generative neural networks that construct a reversible and efficient differentiable mapping (Tong et al. 2024) between a fixed distribution (e.g., standard normal) and the data distribution (Rezende and Mohamed 2015) through exact likelihood estimation. Traditional NFs design this mapping as a static composition of reversible modules, while continuous normalizing flows (CNFs) represent this mapping through neural ODEs (Chen et al. 2018). However, CNFs face challenges in training and handling large datasets (Chen et al. 2018; Grathwohl et al. 2019; Onken et al. 2021). Flow Matching (FM) (Lipman et al. 2023) generates high-quality samples and stabilizes CNFs training, but its reliance on the Gaussian source distribution makes it less convenient for broader applications. CFM (Tong et al. 2024) addresses this problem by extending existing diffusion and FM methods. For example, EquiFM (Song et al. 2024) and MolFlow (Irwin et al. 2024) use CFM for 3D molecular generation, achieving superior performance across multiple molecular generation benchmarks and improving sampling speed.

In this paper, we apply the CFM method to molecular conformation prediction, directly predicting the vector field around molecular atomic coordinates and achieving stable and efficient training.

Invariant and Equivariant Neural Networks

Invariant neural networks model molecules using intermediate geometric variables, including interatomic distances (Simm and Hernandez-Lobato 2020; Xu et al. 2021; Shi et al. 2021) and bond features (Ganea et al. 2021), which are invariant to translation and rotation. These methods avoid directly modeling complex atomic coordinates, but their reliance on intermediate geometric variables limits their flexibility during training or inference.

Equivariant neural networks (Thomas et al. 2018; Thölke and Fabritius 2022; Le, Noé, and Clevert 2022; Liao and Smidt 2023; Liao et al. 2024) operate on type-L vectors and geometric tensors. These models utilize tensor field networks (TFN) (Thomas et al. 2018), which employ spherical harmonics and irreducible representations to ensure three-dimensional translational and rotational equivariance. Methods based on equivariant transformers (Thölke and Fabritius 2022; Le, Noé, and Clevert 2022) used dot product atten-

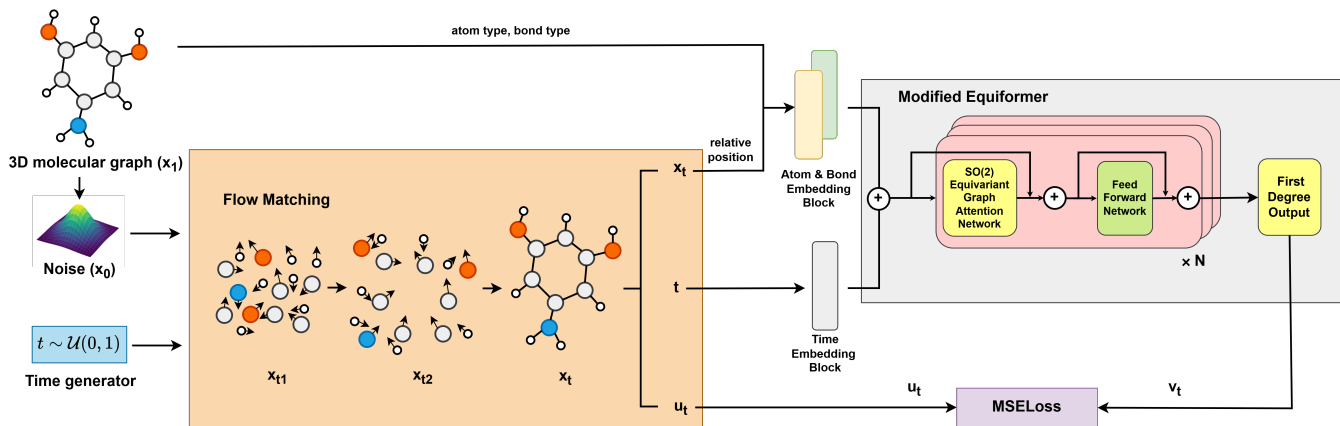


Figure 1: The architecture of ConfromFlow. The architecture involves using fixed atom and bond types as conditions, followed by Flow Matching on the atomic coordinates to produce x_t , t , and u_t . After embedding the relative position features and time features along with the conditions, a modified Equiformer is employed to predict the vector field v_t around the atoms. Using Mean Squared Error (MSE) loss, the predicted vector field v_T is then fitted to the ground truth vector field u_T obtained from Flow Matching. For training procedure, see Algorithm 1, for sampling procedure, see Algorithm 2.

tion (Vaswani et al. 2017) and linear message passing, and adopted a specialized architecture that considered only type-0 and type-1 vectors. Equiformer (Liao and Smidt 2023) integrates MLP attention, non-linear messaging (Gilmer et al. 2017; Sanchez-Gonzalez et al. 2020), and higher-degree vectors to incorporate higher-degree tensor product interactions, achieving enhanced performance. EquiformerV2 (Liao et al. 2024) builds on Equiformer, replacing SO(3) convolutions with eSCN convolutions and optimizing the model architecture to enhance performance in higher-degree contexts.

We enhance the embedding blocks of EquiformerV2 (Liao et al. 2024) to encode Cartesian molecular conformations while ensuring both translational and rotational invariance. This improvement efficiently captures feature information and facilitates effective interaction with higher-degree molecular features.

3D Molecular conformation Prediction

Cheminformatics and deep learning are the two most commonly used approaches for 3D molecular conformation prediction. The former leverages chemical heuristics, rules, and databases to achieve significantly faster generation. However, while these methods efficiently model constrained degrees of freedom, they fall short in capturing the full energy landscape. Notable examples include the commercial software OMEGA (Hawkins et al. 2010) and the open-source RDKit ETKDG (Landrum et al. 2013). On the other hand, deep learning methods exploit molecular structural symmetry to introduce inductive biases, enhancing their predictive capabilities. Examples include GeoMol (Ganea et al. 2021), GeoDiff (Xu et al. 2022), and Torsional Diffusion (Jing et al. 2022).

EquiFlow stands out by effectively simulating the complex distribution of molecular conformations and accurately predicting the 3D structure of molecules.

Methodology

In this section, we first define the problem of predicting the 3D conformation of molecules. Subsequently, we detail the components of EquiFlow, including an equivariant CFM with OT and a modified equiformer. The framework of EquiFlow is illustrated in Figure 1.

Problem Definition

A molecule can be represented as an undirected graph $G = \langle X, E \rangle$, where $X = (X_1, X_2, \dots, X_k) \in \mathbb{R}^{k \times 3}$ denotes the coordinate matrix of k atoms, and $E = (e_{ij}, (i, j) \in |X| \times |X|)$ denotes the feature matrix of the edges between atoms. Our goal is to model the known atomic coordinates of a molecule while keeping the atomic types fixed, in order to accurately predict the 3D conformation of the molecule, encompassing both diversity and accuracy.

Equivariant Conditional Flow Matching with Optimal Transport

Normalizing Flows (NFs). Let x_0 denotes data points from a prior distribution p_0 , and x_1 denotes samples from an output distribution p_1 . NFs (Rezende and Mohamed 2015; Papamakarios et al. 2021) provide a powerful framework for learning complex probability distributions through the concept of invertible transformations ($f_\theta : \mathbb{R}^{k \times 3} \rightarrow \mathbb{R}^{k \times 3}$). It transforms samples from $p_0(x_0)$ to $p_1(x_1)$, known as the forward distribution, and utilizes the change of variables formula:

$$p_1(x_1) = p_0(f^{-1}(x_1)) \left| \det \left(\frac{\partial f_\theta^{-1}(x_1)}{\partial x_1} \right) \right| \quad (1)$$

where $\frac{\partial f_\theta^{-1}(x_1)}{\partial x_1}$ represents the Jacobian matrix of the inverse transformation f_θ^{-1} . In essence, NFs enable the continuous

reshaping of a simpler, known distribution into a more intricate, unknown distribution, while preserving invertibility and allowing for exact likelihood evaluation.

Continuous Normalizing Flows (CNFs). First, we define some notations: the time-dependent probability density path $p_{t \in [0,1]} : \mathbb{R}^{k \times 3} \rightarrow \mathbb{R}_{>0}$, the time-dependent vector field $v_{t \in [0,1]} : \mathbb{R}^{k \times 3} \rightarrow \mathbb{R}^{k \times 3}$, and the time-dependent flow $f_\theta(x, t) : \mathbb{R}^{k \times 3} \times [0, 1] \rightarrow \mathbb{R}^{k \times 3}$. CNFs (Chen et al. 2018) are a class of NFs defined by an ODE:

$$df_\theta(x, t) = v_\theta(f_\theta(x, t), t) dt \quad (2)$$

with the initial condition:

$$f_\theta(x, 0) = x \quad (3)$$

where the time-dependent vector field uniquely determines the time-dependent flow. (Chen et al. 2018) proposed using an ODE solver to train CNFs. However, due to the need for numerical ODE simulation, CNFs are challenging to train.

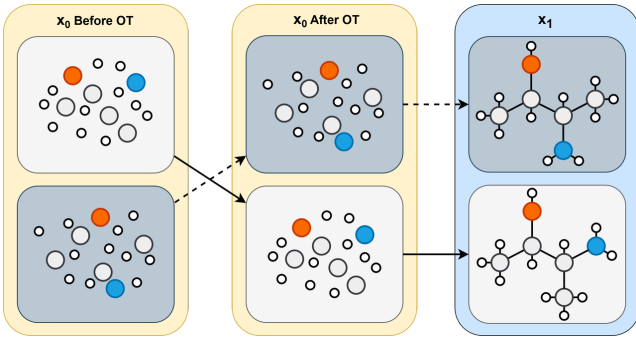


Figure 2: The process of Equivariant OT-CFM. We perform OT between different conformations of the same molecule to obtain the mapping that minimizes the transport cost between the Gaussian noise coordinates x_0 and the true conformation coordinates x_1 . Following this, we calculate the conditional probability path and the corresponding conditional vector field during the CFM process. Note that both x_0 and x_1 need to be centered using the Zero Center-of-Mass (Zero CoM) operation to ensure translational equivariance, and the Kabsch algorithm (Kabsch 1976) is used for rotational alignment.

Optimal Transport Between Conformations. (Lipman et al. 2023) proposed the Flow Matching objective to train CNFs without simulation, regressing the neural network $v_\theta(x, t)$ to a target vector field $u_t(x)$:

$$\mathcal{L}_{\text{FM}}(\theta) = \mathbb{E}_{t, p_t(x)} \|v_\theta(x, t) - u_t(x)\|^2 \quad (4)$$

However, this objective requires prior knowledge of the vector field $u_t(x)$ and the corresponding probability density path $p_t(x)$, which is difficult to achieve.

To address the computational challenges of Flow Matching objectives, it has been shown by (Lipman et al. 2023) that utilizing CFM loss yields gradients equivalent to traditional methods. Moreover, (Tong et al. 2024) has successfully applied CFM loss to achieve effective results (see details in Appendix B):

$$\mathcal{L}_{\text{CFM}}(\theta) = \mathbb{E}_{t, p_t(x|z)} \|v_\theta(x, t) - u_t(x|z)\|^2 \quad (5)$$

where the conditional distribution is defined by the OT map $\pi(x_0, x_1)$, which is determined by the 2-Wasserstein distance:

$$W_2^2 = \inf_{\pi \in \Pi} \int c(x_0, x_1) \pi(dx_0, dx_1) \quad (6)$$

here, Π represents the set of all couplings, and $c(x_0, x_1) = \|x_0 - x_1\|^2$ denotes the squared Euclidean distance used as the cost function to obtain the OT map matrix M .

In this work, we focus on predicting atomic-level features, emphasizing fixed atomic type characteristics while concentrating on the OT mapping (Figure 2) of molecular coordinates x . As seen in Appendix B, previous studies (Lipman et al. 2023; Tong et al. 2024) calculated the squared Euclidean distance between atoms directly as a cost function for the OT map. They then calculated the vector field along a straight line, moving the atomic coordinates directly to the real atomic coordinates. However, this straight-line approach may pose issues in 3D molecular conformation prediction due to the influence of spatial symmetry (see details in Appendix A), which may prevent accurate approximation of the OT mapping in 3D molecular conformation prediction.

To address this issue, we start by considering x_0 as a point cloud sampled from a Gaussian distribution representing molecular coordinates, and x_1 as the point cloud of true molecular coordinates. We first apply the Zero CoM operation to both x_0 and x_1 to ensure translational invariance. We then use the Kabsch algorithm (Kabsch 1976) to find the optimal rotation matrix that aligns x_0 and x_1 ensuring rotational invariance. Instead of using the Euclidean squared distance, we calculate the Root Mean Square Deviation (RMSD) matrix between the aligned molecules as the cost function, the RMSD for each pair of conformation $C(x_{0_i}, x_{1_j})$ is calculated using Equation 7, where K is the number of atoms in the molecule, and x_1 is rotated using the Kabsch algorithm to achieve best alignment with x_0 .

$$C(x_{0_i}, x_{1_j}) = \sqrt{\frac{1}{K} \sum_{k=1}^K \|x_{0_{i_k}} - x_{1_{j_k}}\|^2} \quad (7)$$

We perform OT between different conformations of each molecule. Our Equivariant OT-CFM process is as follows:

1. Initialize the conformation coordinates x_0 to follow a Gaussian distribution based on the conformation coordinates x_1 from the true target distribution p_1 .
2. Calculate the cost matrix using Equation 7 and then obtain the OT map matrix M with the minimal cost.

$$M = \arg \min_{i,j} \sum C(x_{0_i}, x_{1_j}) \quad (8)$$

3. Obtain the molecular coordinate pairs (x_{0_i}, x_{1_j}) that satisfies the OT map matrix M .
4. Compute the conditional probability path $p_t(x|z)$ and conditional vector field $u_t(x|z)$ (see Appendix B) based on the paired molecular coordinates (x_{0_i}, x_{1_j}) .

Modified Equiformer

Equiformer. Equiformer (Liao and Smidt 2023) is a deep learning model that combines the attention mechanism of Transformers with the SE(3) equivariance mechanism of Graph Neural Networks (GNNs). To ensure equivariance, Equiformer substitutes scalar node features with equivariant irreducible representations (irreps) features, performing equivariant operations on these irreps features, and adding equivariant graph attention to message passing. These operations include the depth-wise tensor product (DTP), and equivariant linear operations, equivariant layer normalization (Batzner et al. 2022), and gate activation (Weiler et al. 2018). Furthermore, Equiformer uses nonlinear functions in attention weights and message passing, giving it stronger attention expression capabilities than typical Transformers.

EquiformerV2. Building upon Equiformer, EquiformerV2 (Liao et al. 2024) replaces SO(3) convolutions with eSCN convolutions, enabling more efficient incorporation of higher-degree tensors. The paper introduces three architectural improvements:

1. Attention Re-normalization: By introducing additional layer normalization, it stabilizes the training process when extending to higher degrees.
2. Separable S^2 Activation: Replaces Gate Activation with two-layer MLP, making the training process more stable and enhancing the model’s expressive capability.
3. Separable Layer Normalization: Normalizes different degrees separately, improving the model’s performance in higher degrees.

These improvements make EquiformerV2 more efficient in handling complex three-dimensional atomic systems.

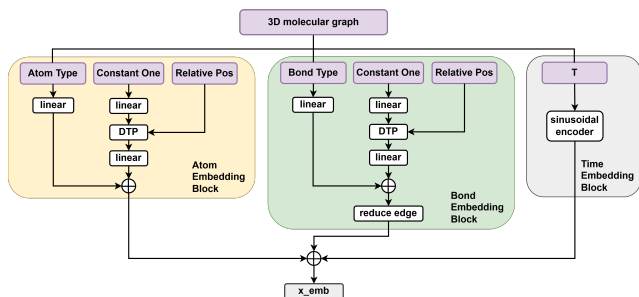


Figure 3: Atom, Bond, and Time Embedding Blocks in Modified Equiformer. We embed input 3D molecular graph with Atom Type, Bond Type, Relative Pos, and Time embeddings before transformer blocks, consisting of SO(2) equivariant graph attention and feed forward networks.

Modified Equiformer. EquiFlow made three modifications to EquiformerV2, adapting it for the FM training framework and tasks like single-conformation prediction and multi-conformation generation. These modifications include:

1. Time Embedding: Adding time embedding $T(t)$ to all degrees and orders of irreps features f , enabling the model

to capture temporal changes in the FM training framework.

$$f_{m,i}^{(L)} = f_{m,i}^{(L)} + T(t)_i \quad (9)$$

2. Edge Feature Calculation: Changing the calculation of edge features from using Gaussian Radial Basis Function (RBF) for adjacent atom distances to using chemical bonds within molecules, allowing the model to better understand the role of chemical bonds.
3. Prediction Head: Modifying the prediction head from aggregated 0-degree feature encoding to non-aggregated 1-degree feature encoding, since atomic 3D coordinates belong to 1-degree features.

Figure 3 shows the embedding x_{emb} used in the modified Equiformer. The embedding is a sum of atom embedding, bond embedding and time embedding. We found that using the atom embedding method to embed bond type features produces a better result than the original equiformer, where bond types are not considered. The modified Equiformer shows improved performance in molecular conformation prediction tasks within the FM training framework.

Algorithm 1: Training Procedure

Require: Let v_θ be the modified Equiformer. Let x be a molecule, with x_c denoting the coordinates of its m conformations $\{x_{c_0}, x_{c_1}, \dots, x_{c_m}\}$. Here, x_α and x_β represent the atom types and bond types, respectively.

- 1: **while** Training **do**
 - 2: $n \leftarrow \min(m, N)$
 - 3: $x_1 \subseteq_{\mathbb{R}} x_c$ where $x_1 = \{x_{1_1}, x_{1_2}, \dots, x_{1_n}\}$
 - 4: $x_0 \sim \mathcal{N}(0, 1)$
 - 5: $t \sim \mathcal{U}(0, 1)$
 - 6: $x_{0_i}, x_{1_j} \leftarrow \text{OT-CFM}(x_0, x_1)$
 - 7: $x_{0_i}, x_{1_j} \leftarrow (x_{0_i} - \text{CoM}(x_{0_i})), (x_{1_j} - \text{CoM}(x_{1_j}))$
 - 8: $u_t \leftarrow x_{1_j} - x_{0_i}$
 - 9: $x_t \leftarrow x_{0_i} + t \cdot u_t$
 - 10: $v_t \leftarrow v_\theta(x_t, x_\alpha, x_\beta, t)$
 - 11: $\mathcal{L}_{\text{CFM}}(\theta) \leftarrow \|v_t - u_t\|^2$
 - 12: $\theta \leftarrow \text{Update}(\theta, \nabla_\theta \mathcal{L}_{\text{CFM}}(\theta))$
 - 13: **end while**
-

Algorithm 2: Sampling Procedure

Require: Let v_θ be the modified Equiformer. Let x be a molecule, with x_α and x_β representing the atom types and bond types, respectively.

- 1: $x_0 \sim \mathcal{N}(0, 1)$
 - 2: $x_0 \leftarrow x_0 - \text{CoM}(x_0)$
 - 3: $x_1 \leftarrow \text{ODESolve}(v_\theta, (x_0, x_\alpha, x_\beta, t), (0, 1))$
-

Training Procedure

In Algorithm 1, each sample x in the training dataset represents a molecule containing m conformations, where m may vary for each molecule. The Cartesian coordinates for the conformations of each molecule are denoted by

Methods	COV-R (%) \uparrow		MAT-R (\AA) \downarrow		COV-P (%) \uparrow		MAT-P (\AA) \downarrow	
	mean	median	mean	median	mean	median	mean	median
RDKit	85.1	100.0	0.235	0.199	86.8	100.0	0.232	0.205
OMEGA	85.5	100.0	0.177	0.126	82.9	100.0	0.224	0.186
GeoMol	91.5	100.0	0.225	0.193	86.7	100.0	0.270	0.241
GeoDiff	76.5	100.0	0.297	0.229	50.0	33.5	0.524	0.510
Torsional diffusion	92.8	100.0	0.178	0.147	92.7	100.0	0.221	0.195
EquiFlow	95.9	100.0	0.130	0.079	91.8	100.0	0.164	0.108

Table 1: Results on the GEOM-QM9 test dataset. EquiFlow outperforms all other methods in several key metrics on the GEOM-QM9 test dataset. It achieves the highest COV-R and the lowest MAT-R, indicating a superior ability to cover diverse conformations. The method also excels in precision-related metrics, with a competitive COV-P and the lowest MAT-P, highlighting its effectiveness in generating highly precise conformations.

$x_c = (x_{c_0}, x_{c_1}, \dots, x_{c_m})$. To ensure balanced training across molecules, we randomly select n conformations from x_c to create x_1 , where

$$n = \begin{cases} N & \text{if } m > N \\ m & \text{else} \end{cases} \quad \text{and} \quad x_1 = (x_{1_1}, x_{1_2}, \dots, x_{1_n}) \quad (10)$$

here, N represents the maximum number of conformations selected for training.

A set of n initial noise coordinates $x_0 = (x_{0_1}, x_{0_2}, \dots, x_{0_n})$ is sampled from a Gaussian distribution $\mathcal{N}(0, 1)$. Additionally, a set $t = (t_1, t_2, \dots, t_n)$ is sampled from a uniform distribution $\mathcal{U}(0, 1)$. x_0 and x_1 are then passed to OT-CFM to create (x_{0_i}, x_{1_j}) pairs according to the cost function $C(x_0, x_1)$. then combined with t to create u_t and x_t such that

$$u_t = x_{1_j} - x_{0_i} \quad \text{and} \quad x_t = x_{0_i} + tu_t \quad (11)$$

Finally, the modified Equiformer v_θ takes x_t along with the atom types and the bond types as input, then outputs v_t to fit u_t using MES loss function. For detailed Hyperparameter settings related to training, please refer to Appendix C.

Sampling Procedure

Algorithm 2 describes the sampling procedure. First, sample x_0 from a Gaussian distribution $\mathcal{N}(0, 1)$. This Gaussian sample is then adjusted using a Zero CoM operation to ensure it has a center of mass at the origin. The modified sample, along with the molecule’s atom types x_α , bond types x_β , and a time interval t , is passed to an ODE solver, which integrates the modified Equiformer model v_θ over the time interval $[0, 1]$ to produce the final sample x_1 .

Experiments

Experimental Setups

Evaluation Tasks. In this section, we evaluate EquiFlow on single-conformation and multi-conformation prediction tasks for small molecules, following the evaluation setup from previous works on 3D molecular conformation (Xu et al. 2022; Jing et al. 2022; Song et al. 2024). The single-conformation prediction task evaluates the accuracy of 3D

conformation predictions on the QM9 dataset. The multi-conformation prediction task comprehensively assesses the accuracy and diversity of 3D conformation predictions on the GEOM-QM9 dataset.

Datasets. For the single-conformation prediction task, EquiFlow employs the QM9 dataset (Ramakrishnan et al. 2014), which comprises 130,831 molecules, each containing up to nine heavy atoms. We remove all hydrogens and split the dataset, resulting in a training set with 100,000 molecules, a validation set with 17,748 molecules, and a test set with 13,083 molecules. For the multi-conformation prediction task, EquiFlow utilizes the GEOM-QM9 (Ramakrishnan et al. 2014) dataset. To facilitate OT between different conformations of the same molecule, we aggregate the dataset by grouping conformations with identical SMILES notations and remove invalid conformations—those with the same SMILES notation but differing in the number or type of chemical bonds. Following the dataset split of Torsional Diffusion (Jing et al. 2022), the final dataset consists of a training set with 106,586 molecules comprising 1,447,427 conformations, a validation set with 13,323 molecules comprising 193,998 conformations, and a test set with 1,000 molecules comprising 13,730 conformations.

Baselines. For the multi-conformation prediction task, we compare our results with those of RDKit, OMEGA, GeoMol, GeoDiff, and Torsional Diffusion, which are directly taken from (Jing et al. 2022).

Evaluation Metrics. For the single-conformation prediction task, we measure the accuracy of the predicted molecular conformations by calculating the RMSD between the predicted molecular coordinates x_p and the true molecular coordinates x_t . For the multi-conformation prediction task, we follow Geodiff (Xu et al. 2022) to calculate the mean and median of four RMSD-based evaluation metrics to assess the diversity and accuracy of the predicted molecular conformations. Let S_p and S_t represent the sets of predicted and true conformations, respectively. The coverage and matching metrics, following the traditional recall and precision

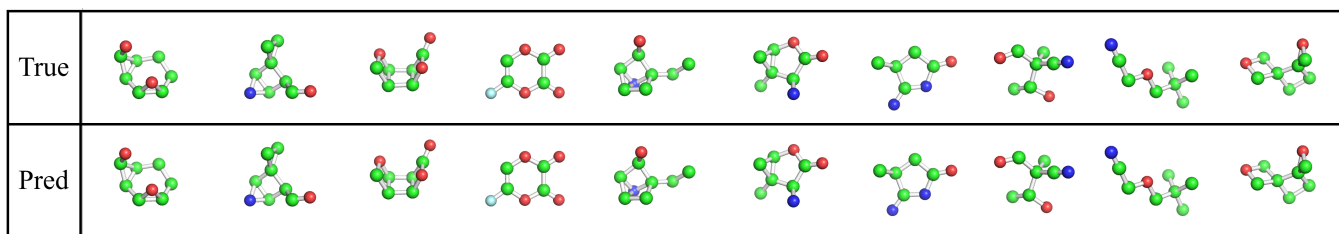


Figure 4: Samples from the single-conformation prediction on QM9 dataset. We selected 10 molecules, with SMILES from left to right as follows: C1CC2(CO2)C12COC2, CC(C)(C)COCC#N, CC(O)C(C)(C#N)C=O, CC1CC(=O)NC1N, CC12CC1OC(=O)C2N, CCC12CC3C(C1O)N32, O=C1OC=C(F)OC1=O, O=C1OC2C3COC3C12, O=CC1C2NC2C12CC2, OC1C2CCC3OC3C12.

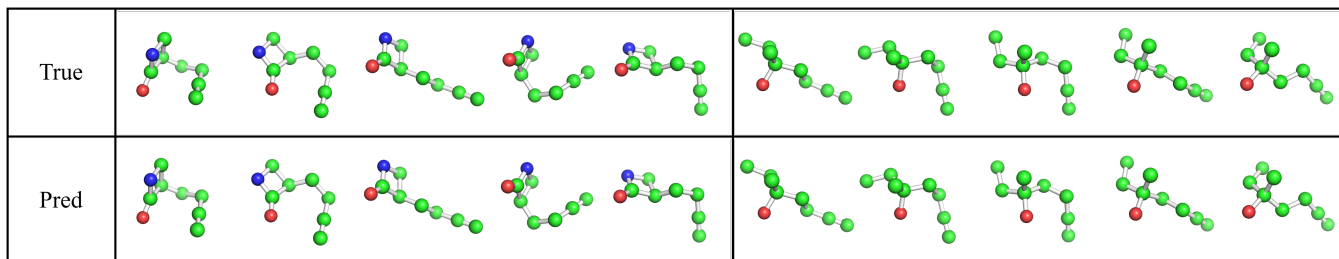


Figure 5: Samples from the multi-conformation prediction on GEOM-QM9 dataset. We selected 5 conformations from 2 molecules for display. The molecule on the left, C#CCC[C@@H]1CNC1=O, consists of 9 conformations in total, while the molecule on the right, C#CCCC@O)CC, has 104 conformations.

measures, can be defined as:

$$\text{COV-R}(S_p, S_t) = \frac{1}{|S_t|} |\{x_t \in S_t \mid \text{RMSD}(x_t, x_p) \leq \delta, x_p \in S_p\}| \quad (12)$$

$$\text{MAT-R}(S_p, S_t) = \frac{1}{|S_t|} \sum_{x_t \in S_t} \min_{x_p \in S_p} \text{RMSD}(x_t, x_p) \quad (13)$$

$$\text{COV-P}(S_p, S_t) = \frac{1}{|S_p|} |\{x_t \in S_p \mid \text{RMSD}(x_t, x_p) \leq \delta, x_p \in S_t\}| \quad (14)$$

$$\text{MAT-P}(S_p, S_t) = \frac{1}{|S_p|} \sum_{x_t \in S_p} \min_{x_p \in S_t} \text{RMSD}(x_t, x_p) \quad (15)$$

where δ is a pre-defined threshold, δ is set as 0.5\AA for the GEOM-QM9 dataset. The size of S_p for each molecule is set to twice the size of S_t . The COV score reflects the percentage of predicted conformations that are deemed successful, where a successful prediction is defined as having an RMSD below the threshold δ . The MAT score calculates the average RMSD between conformations in one set and their nearest counterparts in another. Typically, recall measures diversity, while precision measures accuracy. Higher COV rates or lower MAT scores suggest the prediction is more realistic.

Experimental Results

EquiFlow performed multi-conformation prediction based on the GEOM-QM9 dataset. The prediction results on the test dataset ($\delta = 0.5\text{\AA}$) is shown in Table 1. These results suggest that EquiFlow significantly improves both the diversity and accuracy of molecular conformation predictions compared to other state-of-the-art methods. Apart from multi-conformation prediction, EquiFlow also achieved an excellent RMSD of 0.17\AA on the QM9 test set for single conformations, demonstrating its outstanding ability on both single-conformation and multi-conformation prediction tasks.

Conformation Visualization

To better highlight the performance of EquiFlow, we visualized the predicted molecular conformations for both tasks to provide a qualitative comparison (Figures 4, 5). EquiFlow successfully captures the complex distribution of molecular conformations, achieving accurate predictions while also maintaining state-of-the-art diversity.

Conclusion

We propose EquiFlow, a novel framework for predicting 3D molecular conformations with a focus on accuracy and diversity. The model leverages a combination of Equivariant OT-CFM and a modified Equiformer to handle atomic-level features and 3D spatial symmetry. The incorporation of OT provides a unique approach for mapping molecular conformations, while modifications to the Equiformer architecture enhance performance in tasks involving both single-

conformation and multi-conformation prediction. Our experimental results on the QM9 and GEOM-QM9 datasets demonstrated that EquiFlow achieves state-of-the-art results compared to previous methods, ensuring accurate predictions while maintaining excellent diversity. In future work, we plan to further optimize the model by incorporating the latest advances in CFM methods and extend our approach to conformation prediction for larger molecules.

References

- Batzner, S.; Musaelian, A.; Sun, L.; Geiger, M.; Mailoa, J. P.; Kornbluth, M.; Molinari, N.; Smidt, T. E.; and Kozinsky, B. 2022. E (3)-equivariant graph neural networks for data-efficient and accurate interatomic potentials. *Nature communications*, 13(1): 2453.
- Chen, R. T.; Rubanova, Y.; Bettencourt, J.; and Duvenaud, D. K. 2018. Neural ordinary differential equations. *Advances in neural information processing systems*, 31.
- Ganea, O.; Pattanaik, L.; Coley, C.; Barzilay, R.; Jensen, K.; Green, W.; and Jaakkola, T. 2021. Geomol: Torsional geometric generation of molecular 3d conformer ensembles. *Advances in Neural Information Processing Systems*, 34: 13757–13769.
- Gebauer, N. W.; Gastegger, M.; Hessmann, S. S.; Müller, K.-R.; and Schütt, K. T. 2022. Inverse design of 3d molecular structures with conditional generative neural networks. *Nature communications*, 13(1): 973.
- Gilmer, J.; Schoenholz, S. S.; Riley, P. F.; Vinyals, O.; and Dahl, G. E. 2017. Neural message passing for quantum chemistry. In *International conference on machine learning*, 1263–1272. PMLR.
- Grathwohl, W.; Chen, R. T. Q.; Bettencourt, J.; and Duvenaud, D. 2019. Ffjord: Free-form continuous dynamics for scalable reversible generative models. In *International Conference on Learning Representations*.
- Hawkins, P. C.; Skillman, A. G.; Warren, G. L.; Ellingson, B. A.; and Stahl, M. T. 2010. Conformer generation with OMEGA: algorithm and validation using high quality structures from the Protein Databank and Cambridge Structural Database. *Journal of chemical information and modeling*, 50(4): 572–584.
- Ho, J.; Jain, A.; and Abbeel, P. 2020. Denoising diffusion probabilistic models. *Advances in neural information processing systems*, 33: 6840–6851.
- Hoogeboom, E.; Satorras, V. G.; Vignac, C.; and Welling, M. 2022. Equivariant diffusion for molecule generation in 3d. In *International conference on machine learning*, 8867–8887. PMLR.
- Irwin, R.; Tibo, A.; Janet, J.-P.; and Olsson, S. 2024. Efficient 3D Molecular Generation with Flow Matching and Scale Optimal Transport. *arXiv preprint arXiv:2406.07266*.
- Jing, B.; Corso, G.; Chang, J.; Barzilay, R.; and Jaakkola, T. 2022. Torsional diffusion for molecular conformer generation. *Advances in Neural Information Processing Systems*, 35: 24240–24253.
- Jing, B.; Eismann, S.; Suriana, P.; Townshend, R. J. L.; and Dror, R. 2020. Learning from protein structure with geometric vector perceptrons. In *International Conference on Learning Representations*.
- Kabsch, W. 1976. A solution for the best rotation to relate two sets of vectors. *Acta Crystallographica Section A: Crystal Physics, Diffraction, Theoretical and General Crystallography*, 32(5): 922–923.
- Landrum, G.; et al. 2013. RDKit: A software suite for cheminformatics, computational chemistry, and predictive modeling. *Greg Landrum*, 8(31.10): 5281.
- Le, T.; Noé, F.; and Clevert, D.-A. 2022. Equivariant graph attention networks for molecular property prediction. *arXiv preprint arXiv:2202.09891*.
- Li, X.; Thickstun, J.; Gulrajani, I.; Liang, P. S.; and Hashimoto, T. B. 2022. Diffusion-lm improves controllable text generation. *Advances in Neural Information Processing Systems*, 35: 4328–4343.
- Liao, Y.-L.; and Smidt, T. 2023. Equiformer: Equivariant Graph Attention Transformer for 3D Atomistic Graphs. In *The Eleventh International Conference on Learning Representations*.
- Liao, Y.-L.; Wood, B. M.; Das, A.; and Smidt, T. 2024. EquiformerV2: Improved Equivariant Transformer for Scaling to Higher-Degree Representations. In *The Twelfth International Conference on Learning Representations*.
- Lipman, Y.; Chen, R. T. Q.; Ben-Hamu, H.; Nickel, M.; and Le, M. 2023. Flow Matching for Generative Modeling. In *The Eleventh International Conference on Learning Representations*.
- Onken, D.; Fung, S. W.; Li, X.; and Ruthotto, L. 2021. Ot-flow: Fast and accurate continuous normalizing flows via optimal transport. In *Proceedings of the AAAI Conference on Artificial Intelligence*, volume 35, 9223–9232.
- Papamakarios, G.; Nalisnick, E.; Rezende, D. J.; Mohamed, S.; and Lakshminarayanan, B. 2021. Normalizing flows for probabilistic modeling and inference. *Journal of Machine Learning Research*, 22(57): 1–64.
- Ramakrishnan, R.; Dral, P. O.; Rupp, M.; and Von Lilienfeld, O. A. 2014. Quantum chemistry structures and properties of 134 kilo molecules. *Scientific data*, 1(1): 1–7.
- Rezende, D.; and Mohamed, S. 2015. Variational inference with normalizing flows. In *International conference on machine learning*, 1530–1538. PMLR.
- Rombach, R.; Blattmann, A.; Lorenz, D.; Esser, P.; and Ommer, B. 2022. High-resolution image synthesis with latent diffusion models. In *Proceedings of the IEEE/CVF conference on computer vision and pattern recognition*, 10684–10695.
- Sanchez-Gonzalez, A.; Godwin, J.; Pfaff, T.; Ying, R.; Leskovec, J.; and Battaglia, P. 2020. Learning to simulate complex physics with graph networks. In *International conference on machine learning*, 8459–8468. PMLR.
- Satorras, V. G.; Hoogeboom, E.; and Welling, M. 2021. E (n) equivariant graph neural networks. In *International conference on machine learning*, 9323–9332. PMLR.

Shi, C.; Luo, S.; Xu, M.; and Tang, J. 2021. Learning gradient fields for molecular conformation generation. In *International conference on machine learning*, 9558–9568. PMLR.

Simm, G.; and Hernandez-Lobato, J. M. 2020. A Generative Model for Molecular Distance Geometry. In *International Conference on Machine Learning*, 8949–8958. PMLR.

Sohl-Dickstein, J.; Weiss, E.; Maheswaranathan, N.; and Ganguli, S. 2015. Deep unsupervised learning using nonequilibrium thermodynamics. In *International conference on machine learning*, 2256–2265. PMLR.

Song, Y.; and Ermon, S. 2019. Generative modeling by estimating gradients of the data distribution. *Advances in neural information processing systems*, 32.

Song, Y.; Gong, J.; Xu, M.; Cao, Z.; Lan, Y.; Ermon, S.; Zhou, H.; and Ma, W.-Y. 2024. Equivariant flow matching with hybrid probability transport for 3d molecule generation. *Advances in Neural Information Processing Systems*, 36.

Tabak, E. G.; and Turner, C. V. 2013. A family of nonparametric density estimation algorithms. *Communications on Pure and Applied Mathematics*, 66(2): 145–164.

Tabak, E. G.; and Vanden-Eijnden, E. 2010. Density estimation by dual ascent of the log-likelihood. *Communications in Mathematical Sciences*, 8(1): 217–233.

Thomas, N.; Smidt, T.; Kearnes, S.; Yang, L.; Li, L.; Kohlhoff, K.; and Riley, P. 2018. Tensor field networks: Rotation-and translation-equivariant neural networks for 3d point clouds. *arXiv preprint arXiv:1802.08219*.

Thölke, P.; and Fabritius, G. D. 2022. Equivariant Transformers for Neural Network based Molecular Potentials. In *International Conference on Learning Representations*.

Tong, A.; FATRAS, K.; Malkin, N.; Huguet, G.; Zhang, Y.; Rector-Brooks, J.; Wolf, G.; and Bengio, Y. 2024. Improving and generalizing flow-based generative models with minibatch optimal transport. *Transactions on Machine Learning Research*. Expert Certification.

Vaswani, A.; Shazeer, N.; Parmar, N.; Uszkoreit, J.; Jones, L.; Gomez, A. N.; Kaiser, Ł.; and Polosukhin, I. 2017. Attention is all you need. *Advances in neural information processing systems*, 30.

Wang, J.; Wolf, R. M.; Caldwell, J. W.; Kollman, P. A.; and Case, D. A. 2004. Development and testing of a general amber force field. *Journal of computational chemistry*, 25(9): 1157–1174.

Weiler, M.; Geiger, M.; Welling, M.; Boomsma, W.; and Cohen, T. S. 2018. 3d steerable cnns: Learning rotationally equivariant features in volumetric data. *Advances in Neural Information Processing Systems*, 31.

Xu, M.; Wang, W.; Luo, S.; Shi, C.; Bengio, Y.; Gomez-Bombarelli, R.; and Tang, J. 2021. An end-to-end framework for molecular conformation generation via bilevel programming. In *International conference on machine learning*, 11537–11547. PMLR.

Xu, M.; Yu, L.; Song, Y.; Shi, C.; Ermon, S.; and Tang, J. 2022. GeoDiff: A Geometric Diffusion Model for Molecular Conformation Generation. In *International Conference on Learning Representations*.

A. 3D Molecular Symmetry Problem

SE(3)-Equivariant and Irreducible Representations(irreps)

For any input $x \in X$, output $y \in Y$, and group element $g \in G$, if the condition $f(D_X(g)x) = D_Y(g)f(x)$ is satisfied, then we call the function f equivariant. Here, X and Y are vector spaces, f is a mapping function between them, and $D_X(g)$ and $D_Y(g)$ are the transformation matrices parameterized by g in X and Y . In the context of 3D atomic graphs, we specifically focus on the special Euclidean group $SE(3)$, which arises from 3D translations and rotations. In this case, the input features and the learnable functions possess $SE(3)$ -Equivariant properties. Specifically, the transformations $D_X(g)$ and $D_Y(g)$ can be represented by a translation t and an orthogonal matrix R that denotes a rotation or reflection. When these transformations are applied to the input, if the output undergoes the corresponding equivalent transformation, satisfying $Rf(x) = f(Rx)$, then we call the function f equivariant with respect to the rotation or reflection R .

For the three-dimensional Euclidean group $SE(3)$, under translation and rotation transformations, vectors change with rotation while scalars remain invariant. To address translational symmetry, we follow (Xu et al. 2022) and use the Zero Center-of-Mass(Zero CoM) Operation. For rotational equivariance, it is necessary to introduce the irreducible representations of $SO(3)$, which are the irreducible representations of rotations.

In a given vector space, any representation of the $SO(3)$ group can be decomposed into a series of minimal, indivisible transformation matrices, called irreducible representations (irreps). Specifically, for a group element $g \in SO(3)$, there exists an irreducible matrix $D_L(g)$ of dimension $(2L+1) \times (2L+1)$ (also known as the Wigner-D matrix), which acts on a $(2L+1)$ -dimensional vector space. These irreducible representations are indexed by non-negative integers $L = 0, 1, 2, \dots$, with the L -th degree irreducible representation having a dimension of $(2L+1)$. Here, L can be interpreted as an angular frequency, which determines the rate of change of the vector in the rotating coordinate system. The $D_L(g)$ for different L acts on independent vector spaces. The vectors transformed by $D_L(g)$ are called L -degree vectors. Specifically, $L = 0$ (dimension 1) corresponds to a scalar; $L = 1$ (dimension 3) corresponds to a vector; $L = 2$ (dimension 5) corresponds to a second-degree vector. The elements of an L -degree vector $f^{(L)}$ are indexed by the integer m , denoted as $f_m^{(L)}$ (with m ranging from $-L \leq m \leq L$).

If multiple L -degree vectors are concatenated, they form irreducible features with $SE(3)$ -equivariance. Generally, these irreducible features can be represented as $f_{c,m}^{(L)}$, where $0 \leq L \leq L_{\max}$, $0 \leq c \leq C_L - 1$, and C_L denotes the number of channels for the L -degree vector. This means that in each L -degree vector, there are C_L different vectors, each containing m elements. Different channels of the L -degree vectors are parameterized by different weights but transformed using the same $D_L(g)$. Significantly, conventional scalar features correspond to 0-degree vectors.

Spherical Harmonics and Tensor Product

Spherical Harmonics (SH) achieve the mapping from the unit sphere to the irreducible representation D^l , which can be expressed by the function $Y^{(L)}$. Using spherical harmonics, a vector \vec{r} in the Euclidean space \mathbb{R}^3 can be mapped to an L -degree vector $f^{(L)}$, i.e., $f^{(L)} = Y^{(L)}\left(\frac{\vec{r}}{\|\vec{r}\|}\right)$. $SE(3)$ -Equivariant networks update irreducible features by passing messages of transformed irreducible features between nodes. To interact different L -type vectors during the message-passing process, we use the Tensor Product, which extends multiplication to equivariant invariant features (Liao and Smidt 2023). In $SO(3)$, the tensor product combines an L_1 -degree vector $f^{(L_1)}$ and an L_2 -degree vector $g^{(L_2)}$ using CG (Clebsch-Gordan) coefficients to generate an L_3 -degree vector $h^{(L_3)}$:

$$h_{m_3}^{(L_3)} = (f^{(L_1)} \otimes g^{(L_2)})_{m_3} \quad (16)$$

$$(f^{(L_1)} \otimes g^{(L_2)})_{m_3} = \sum_{m_1=-L_1}^{L_1} \sum_{m_2=-L_2}^{L_2} C_{(L_1, m_1)(L_2, m_2)}^{(L_3, m_3)} \times f_{m_1}^{(L_1)} g_{m_2}^{(L_2)} \quad (17)$$

where m_1 , m_2 , and m_3 represent the order, corresponding to the m_1 -th, m_2 -th, and m_3 -th elements of $f^{(L_1)}$, $g^{(L_2)}$, and $h^{(L_3)}$, respectively. The CG coefficients are non-zero only when $|L_1 - L_2| \leq L_3 \leq |L_1 + L_2|$, which constrains the type of the output vector. Thus, the type of $h^{(L_3)}$ depends on the types of $f^{(L_1)}$ and $g^{(L_2)}$. For example, when $f^{(L_1)}$ is a scalar (i.e., $L_1 = 0$) and $g^{(L_2)}$ is a vector ($L_2 = 1$), $h^{(L_3)}$ is a vector ($L_3 = 1$) formed by the product of $f^{(L_1)}$ and $g^{(L_2)}$.

B. Conditional Flow Matching with Optimal Transport

Where the conditional vector field $u_t(x|z)$ and conditional probability path $p_t(x|z)$ yield the vector field $u_t(x)$ and the corresponding probability path $p_t(x)$:

$$p_t(x) = \int p_t(x|z)p(z) dz \quad (18)$$

$$u_t(x) = \int \frac{p_t(x|z)u_t(x|z)}{p_t(x)} p(z) dz \quad (19)$$

Here, $p(z)$ is an arbitrary conditional distribution independent of x and t . For detailed derivations, refer to (Lipman et al. 2023; Tong et al. 2024). Following the methodology in (Tong et al. 2024), $u_t(x|z)$ and $p_t(x|z)$ are parameterized as:

$$z = (x_0, x_1) \quad \text{and} \quad p(z) = \pi(x_0, x_1) \quad (20)$$

$$u_t(x|z) = x_1 - x_0 \quad (21)$$

$$p_t(x|z) = \mathcal{N}(x | t \cdot x_1 + (1-t) \cdot x_0, \sigma^2) \quad (22)$$

Hyper-parameters	Value
Number of Transformer blocks	6
Maximum degree	[6]
Sigma of cfm	0.0
Remove hydrogen	true
Optimizer	AdamW
Single-conformation	
Flow matcher	cfm
Train batch size	256
Eval batch size	256
Learning rate	0.0005
Weight decay	0.005
Multi-conformation	
Sample coefficient	2
Flow matcher	otcfm
Train batch size	128
Eval batch size	32
Maximum number of conformations	20
RMSD threshold for coverage	0.5
Learning rate	0.001
Weight decay	0.005

Table 2: Hyper-parameters for the single-conformation and multi-conformation prediction tasks.

C. Experimental Details

In this section, we introduce the details of our experiments. We first obtain the feature information of the 3D molecular graph, including atom types, bond types, and coordinates x_1 . Next, we generate a Gaussian initial coordinate x_0 . FM is then performed between x_0 and x_1 to obtain the time-dependent probability path x_T and the corresponding vector field u_T . Finally, we design a Modified Equiformer network to regress this vector field. All hyper-parameters in training of EquiFlow are summarized in Table 2.